J. C. Chastang

Optical Techniques for Measurement of Chamber Spacing

Abstract: Two optical methods were investigated for accurately measuring the gap, or chamber spacing, that separates two closely spaced transparent plates. The first method uses a special microscope in which the main feature is a unit-magnification catadioptric system that gives an aberration-free image of the chamber outside the plates, where it is accessible to a high-power objective. The second method is based upon the light section principle, whereby the image of a slit is projected onto the boundaries of the chamber and is thus doubled. The reflected images are observed with a microscope and the degree of separation, which is proportional to the chamber spacing, is measured. Accuracy better than 2 μm is obtained for the two techniques. The choice of the appropriate method depends on the surface quality of the chamber boundaries.

Introduction

One of the critical dimensional parameters of a class of devices in which the configuration includes two closely spaced glass plates is the distance, or "chamber" spacing, separating these plates. The chamber spacing, which is very small (typically a few hundred micrometers) compared with the thickness of the plates (typically a few millimeters), is to be determined with accuracy of two percent or better. We have investigated the possibility of using optical techniques to solve this problem in the case for which the plates are transparent and isotropic. The simplest solution would seem to be to focus a microscope successively on the upper and lower boundaries of the chamber and to measure the distance between the two settings. In general, however, this solution is impractical. The accuracy of each setting is limited by the depth of focus of the microscope objective being used, a good accuracy in the setting requiring a high numerical aperture. However, a glass viewing plate of appreciable thickness is necessarily present between the chamber and the objective and, even assuming that a high numerical aperture objective of the suitable working distance could be found, the severe aberration introduced by this plate prevents the use of the conventional microscope.

To give an idea of the magnitude of the aberrations and their effect on the depth of focus, we examine the case of spherical (on-axis) aberration. A plane-parallel glass plate normal to the axis of a converging light beam necessarily introduces spherical aberration. If the beam was converging to a single point prior to the interposition of the plate, the convergence will be altered afterwards. Depending upon their inclination, the rays will then converge toward different points. In Fig. 1 the distance P_0P is given by [1]

$$P_0P = [t(n^2 - 1)\sin^2 i]/2n^3, \qquad (1)$$

where P_0 is the point at which the rays converge when their inclination tends toward zero, P is the point at which the rays converge when their inclination is i, t is the plate thickness and n its index of refraction. The corresponding wavefront deformation Δ is expressed by

$$\Delta = [t(n^2 - 1)\sin^4 i]/8n^3. \qquad (2)$$

The maximum value of Δ that can be tolerated is one wavelength, λ, which is conventionally 0.5 μm [2]. The maximum value of sin i is the numerical aperture (N.A.) of the beam. We therefore have the inequality

$$\text{N.A.} \leq [8n^3\lambda/t(n^2 - 1)]^{\frac{1}{4}}. \qquad (3)$$

The depth of focus d of a microscope is given by [3]

$$d = \tfrac{1}{2}\lambda(\text{N.A.})^2, \qquad (4)$$

where N.A. is now the numerical aperture of the objective. Replacing the quantity N.A. by its expression derived from (3), we find

$$d \geq \tfrac{1}{4}[\lambda t(n^2 - 1)/2n^3]^{\frac{1}{2}}. \qquad (5)$$

With the following typical values, $t = 6.25$ mm, $\lambda = 0.5$ μm and $n = 1.5$, we obtain $d \geq 6.5$ μm.

Since two focusing operations are required for a given measurement the maximum error on the chamber spacing would be 12 μm. This is unacceptable; the error on

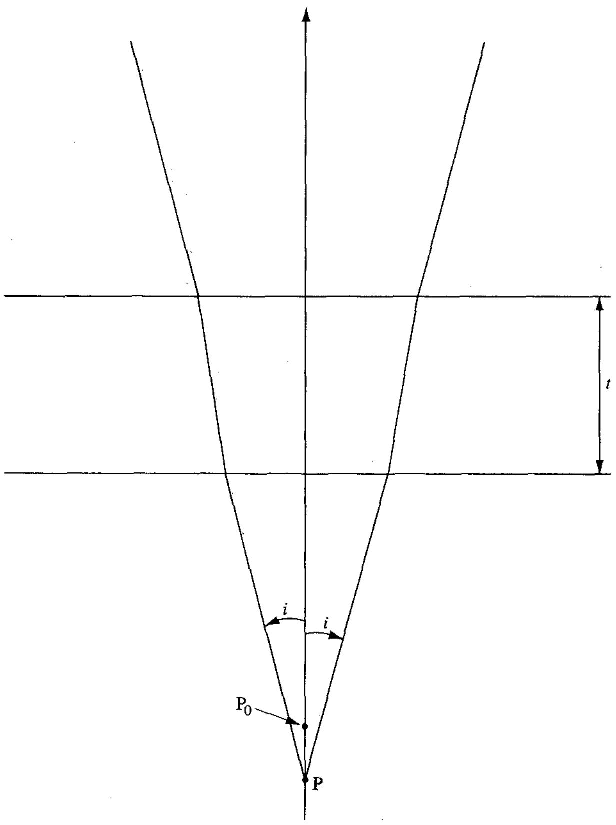

Figure 1 Spherical aberration introduced by a plane-parallel plate in a converging beam.

every measurement cannot exceed a few micrometers. It is theoretically possible to design a microscope objective that will compensate for the aberration introduced by the glass plate. However, this would be an involved and costly solution; moreover, compensation for aberration could be made only for a given plate thickness, thereby limiting the range of application of this objective.

We therefore had to look for alternatives to using a conventional microscope. We have investigated two different schemes. The first uses an aberration-free catadioptric system in conjunction with a suitably modified microscope, and the second is based upon the principle of the light section microscope.

Aberration-free catadioptric system

• *Principle*

Our device results from the adaptation of one described originally by Dyson [4] for the examination of nuclear plates. An almost identical device was reported shortly afterward by Françon [5] for phase-contrast applications. We have found that this device has a remarkable property of self-compensating aberration. This property, not mentioned in Refs. 4 or 5, is discussed here subsequently.

The device consists of a glass hemisphere sectioned along the 30° latitude plane, as shown in Fig. 2. The curved surface of the upper half is coated with a high-reflectivity layer except for a small region surrounding the pole, which is left transparent. One of the plane surfaces resulting from the sectioning is coated with a semitransparent layer, and a small opaque dot is deposited at the center of the other surface. The two halves are then cemented together. A point source coincident with the center of the hemisphere is imaged at the pole without aberration. This occurs because of the stigmatic properties of 1) a spherical mirror used at its center of curvature and 2) a plane mirror. The region of the equatorial plane that lies in the vicinity of the center is imaged aplanetically at the pole without magnification. The purpose of the opaque dot is to prevent rays of very low inclination from reaching the pole region directly, which would create an unwanted background.

An interesting property of the device described here is that a point source located below the equatorial plane in the vicinity of the center, in air or in a medium of refractive index very close to one, is imaged in the vicinity of the pole without magnification or significant aberration. The configuration that leads to this important property is indicated in Fig. 3.

The point B is located immediately under the equatorial plane on the axis of the hemisphere. The ratio of CB to R, where R is the radius of curvature of the hemisphere, is assumed to be small, i.e., no greater than 0.01. Points B_1, B_2, B_3 and B′ are successive images of B in the system. The angles i and r are respectively the angles of incidence and refraction of a ray originating from B. The corresponding angles at the poles x and y differ from r and i only by very small quantities. The locations of the points B_1, B_2, B_3 and B′ given by

$$\begin{aligned} CB_1 &= CB(\tan i/\tan r), \\ CB_2 &\approx CB_1, \\ SB_3 &= CB_2, \\ SB' &\approx SB_3(\tan x/\tan y), \\ &= CB(\tan i \tan x/\tan r \tan y) \approx CB. \end{aligned}$$

The refraction at the pole cancels the aberration introduced by the refraction at the equatorial plane. The above relations are somewhat simplified. The exact paraxial relationship between the line segments SB′ and CB is

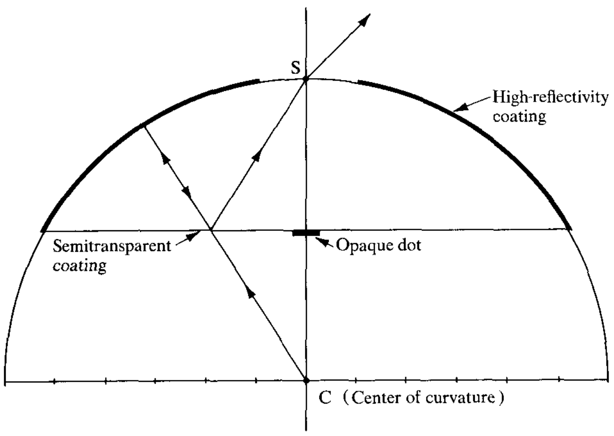

Figure 2 Unit-magnification aberration-free catadioptric system, or hemisphere. A point source located at the center of curvature is imaged at the pole without aberration.

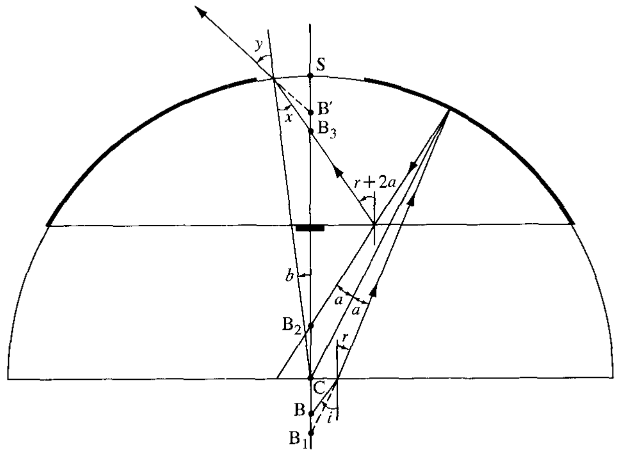

Figure 3 Configuration showing how point B is imaged at point B′ without aberration and with unit magnification. See Eqs. (6) and (7) in text.

$$\mathrm{CB} = \mathrm{SB}'/[1 - (n+1)(\mathrm{SB}'/R)] \approx \mathrm{SB}'[1 + (n+1)(\mathrm{SB}'/R)], \tag{6}$$

where n is the index of refraction of the hemisphere. The exact magnification M of the system is given by the formula

$$M = 1/[1 + (n+1)(\mathrm{CB}/R)] \approx 1 - (n+1)(\mathrm{CB}/R). \tag{7}$$

With $n = 1.5$, and because $\mathrm{CB}/R < 0.01$, M cannot be smaller than 0.975 and therefore differs little from one. Formula (6) should be used to derive the true value of the chamber spacing from experimental measurements. Our calculations indicate that as long as $\mathrm{CB}/R < 0.01$, the maximum value of the corresponding spherical wavefront aberration remains smaller than 0.3 μm (for N.A. = 0.65 and $R = 30$ mm) and may well be considered negligible (see, e.g., [2]). The off-axis contribution from other aberrations may be neglected because of the small field corresponding to a microscope objective with a high numerical aperture.

Implementation

The practical implementation of the system described in the previous section is illustrated in Fig. 4. The hemisphere has been reduced in size and truncated to accommodate the upper glass plate of the device undergoing measurement. For convenience we use the word hemisphere for our system, although it is actually a truncated configuration. The index of refraction of the hemisphere should be very close to the index of the glass plates. The equatorial plane of the hemisphere must be coincident with the upper boundary of the chamber. This geometry must be followed because it is only in this configuration that the aberrations of the system are negligible, as we have established in the previous paragraph. This configuration is achieved by interposing a film of optical immersion oil of the appropriate index between the upper plate of the device and the hemisphere. The oil film allows index matching between the device and the hemisphere; in addition its variable thickness permits the precise positioning of the chamber with respect to the hemisphere. In addition, small variations of the glass plate thickness can be accommodated by changing the oil film thickness accordingly.

In this configuration the portion of the upper boundary, now coincident with the equatorial plane of the hemisphere and located in the vicinity of the center of curvature, is imaged at the pole. The portion of the lower boundary, which is located just under the center of curvature, is also imaged immediately under the pole. The boundaries of the chamber are now imaged with no or negligible aberrations in a location where they are accessible to a microscope equipped with an objective having a high numerical aperture and a short working distance. The distance between the images of the boundaries can be measured with great accuracy and the true value of the chamber spacing can be derived from formula (1).

It should be noted that the glass plate is merely a component in a total system whose main property is to have virtually no aberration, at least if used in the conditions specified. Aside from variations in homogeneity, the plate by itself cannot introduce any aberration into this configuration. We conclude that the imaging of the upper boundary is inherently aberration-free and that the aberrations that occur in the imaging of the lower boundary are self-compensating.

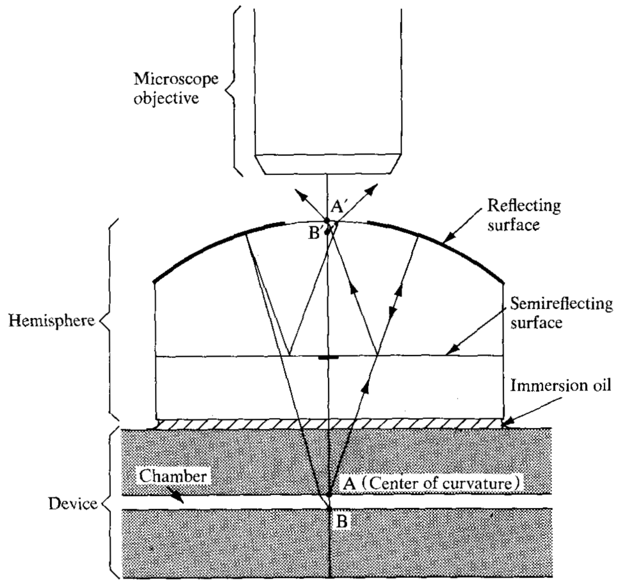

Figure 4 Actual implementation of the hemisphere. The upper boundary of the chamber is coincident with the center of curvature. The chamber is reimaged in the vicinity of the pole with unit magnification and without aberration.

• *Practical considerations*

It is not possible to use the hemisphere in conjunction with an ordinary commercial transmission microscope. In modern microscopes the optical system is usually stationary whereas the sample stage can move up and down. To take advantage of the properties of the hemisphere, both the microscope and the sample stage must be able to move with respect to the hemisphere, which remains stationary. For measurement of the chamber spacing of a given device, the correct procedure includes three distinct operations:

1. The microscope must be focused on the pole of the hemisphere. This is accomplished by a displacement of the microscope.
2. The upper boundary of the chamber must be brought into coincidence with the equatorial plane of the hemisphere so that the image of the upper boundary of the chamber is coincident with the pole. This is accomplished by a displacement of the sample stage, the microscope remaining stationary.
3. The microscope is focused on the image of the lower boundary. This is accomplished by a displacement of the microscope, the sample stage remaining stationary. The displacement of the microscope during this operation gives the chamber spacing.

During all three operations, the hemisphere remains stationary. A special optical configuration has been built which incorporates the hemisphere and the required microscope and sample stage motions. We have used, as much as possible, commercially available components in order to minimize the number of parts that would have to be made or modified.

The hemisphere is a simple optical component that presents no fabrication problem. The major requirement is, of course, that any aberration introduced by the imperfections of the reflecting surfaces be negligible. In order to achieve this, the tolerance on the maximum departure of the actual spherical and planar surfaces from their ideal shapes is set at ± 250 Å. The hemisphere housing is located between the sample stage and the microscope. The displacement of the microscope during the third operation of the procedure described here is monitored by an electronic linear displacement gauge affixed to the head of the instrument column. Although it would theoretically have been possible to use a higher numerical aperture, we have for practical reasons chosen an objective with N.A. = 0.65. The corresponding depth of focus in 0.6 μm.

Implicit in this scheme is the assumption that the chamber boundaries may be focused upon and are observable in some fashion, for example, by patterns deposited on the surfaces or by minute imperfections. If this is not the case the chamber boundaries are invisible under normal conditions in ordinary bright field illumination. The light section method described in the next section allows us to circumvent this difficulty.

Light section microscope

• *Principle*

Figure 5 illustrates the configuration of the light section microscope and its operating principle as applied to our problem. The microscope consists of two optical systems. The plane defined by the intersecting axes of these systems constitutes the plane of symmetry of the total system. The first system includes a light source that illuminates a very narrow slit S perpendicular to the plane of symmetry and a low power microscope objective O_1. The second system includes a low magnification microscope (objective O_2) equipped with a micrometer eyepiece. The device in which the chamber spacing is to be measured is placed perpendicular to the plane of symmetry in such a position that it makes an angle of 45° with the axes of the two previous optical systems. The slit S is projected by means of O_1 into the chamber or close to it. The image S is doubled because of reflection of the incident beam on the upper and lower boundaries. Images S′ and S″ are observed with the microscope, and their lateral separation d, which is proportional to the chamber spacing, is measured with the micrometer.

Because we use a configuration having a plane of symmetry rather than an axis of symmetry, and because a plane-parallel glass plate of appreciable thickness is

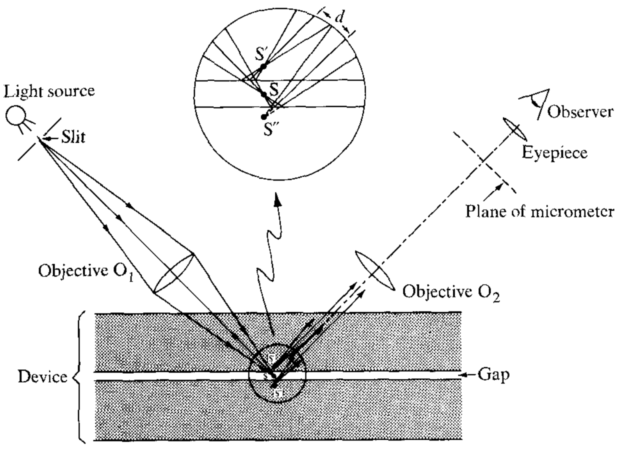

Figure 5 Configuration of a light section microscope. The slit image is doubled by reflections at the gap surfaces, permitting measurement of distance d. Refraction has been omitted for clarity.

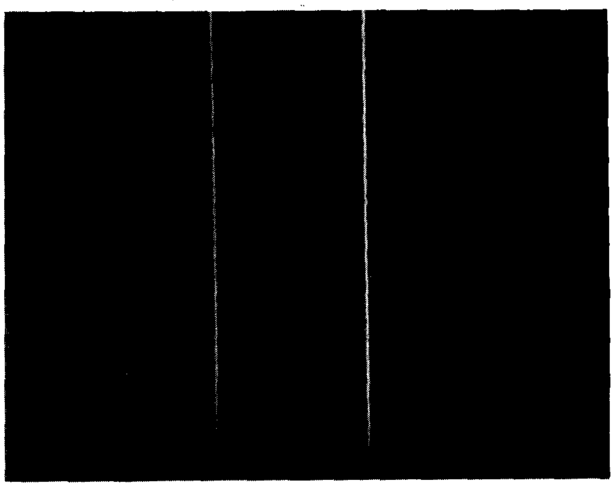

Figure 6 Appearance of the field of view of the light section microscope. Provided that the numerical aperture of the system is sufficiently low, the tangential images of the slit are of good quality. Chamber spacing in this case is 300 μm.

interposed between the measured layer and the other components, large aberration is introduced. The glass plate becomes another component of the total system, as was the case in the previous scheme. The more prominent of these aberrations is astigmatism. If the other aberrations and the image doubling resulting from the two reflections on the boundaries of the chamber are neglected, any point along the slit will be imaged in two different locations: as a small line in the plane of symmetry (sagittal image) in the first and as a small line perpendicular to the plane of symmetry (tangential image) in the second. The sagittal and tangential images of the whole slit consist in the summation of the elementary contributions of all the points along the slit. Taking into account the fact that the slit is perpendicular to the plane of symmetry, only the tangential image will still appear as a narrow line. We therefore deal only with tangential images. It can be shown that the lateral and longitudinal distances d and t between S′ and S″ are given by $d = s\sqrt{2}$ and $t = 2s\sqrt{2}$, in which s is the chamber spacing.

The quantity t is in general of the order of several hundred micrometers and since, to measure the quantity d the appearance of S′ and S″ must be identical, the depth of focus of the total system should be about $t/2$ and its numerical aperture (which is equal to the smallest numerical aperture of either O_1 or O_2) should be quite low. For example, a numerical aperture of 0.03 allows us to deal with values of the chamber spacing up to 300 μm. Under these conditions the remaining aberrations, in particular the on-axis coma, are negligible. With such a small numerical aperture, diffraction broadening of the images of the slit is quite apparent. Instead of measuring the distance between two narrow lines, one has to measure the distance between the center lines of two diffraction patterns. However, since the diffraction patterns are symmetrical, the positions of the center lines can be determined with a high degree of accuracy using the micrometer eyepiece. Provided the linear magnification of the objectives O_1 and O_2 is sufficiently low, for example 5×, the large depth of focus will not induce any significant change in the overall magnification of the system and the magnification may thus be considered constant.

• *Practical considerations*

The simple procedures of the light section method do not require any detailed explanation. The width of the images of the slit for a numerical aperture of 0.03 is about 20 μm. The location of the center lines of these images may be ascertained with any accuracy of 1.5 μm. The corresponding accuracy in the determination of the position of the chamber boundaries is 1 μm. Figure 6 represents an example of the field of view of the microscope, obtained with a bench model of the instrument, while making a measurement. The chamber spacing corresponding to the photograph is about 300 μm. Apparent from this photograph is the fact that the light section method requires very smooth chamber boundaries. Imperfections in these surfaces will broaden, blur or distort the images of the slit, altering the accuracy accordingly.

Summary

We have investigated two optical methods for accurately measuring the gap, or chamber spacing, that separates two closely spaced, plane-parallel glass plates. The first method uses a catadioptric, aberration-free system in conjunction with a specially modified microscope. The

second method consists in an adaptation of the principle of the light section microscope. The accuracies of the two methods are comparable: about 1 μm for the first and 2 μm for the second, for a given chamber spacing measurement. The second method is the simpler procedure. Both techniques require somewhat sophisticated instruments. One main difference between the two methods, however, is the fact that the first requires that the chamber boundaries have markings or structure to permit observation during measurement, whereas the second requires that the chamber boundaries be perfectly smooth.

Acknowledgments

The suggestions and constant assistance of Melvin Klein and Robert Rohr are gratefully appreciated. We are deeply indebted to Michael Costa of the Kingston laboratory for his cooperation and for many helpful suggestions, particularly regarding the light section microscope. We thank Janusz Wilczynski for useful comments.

References

1. M. Bruhat and A. Maréchal, *Optique Geometrique*, Masson et Cie, Paris, 1956, p. 44.
2. M. Born and E. Wolf, *Principles of Optics*, 3rd ed., Pergamon Press, New York, 1965, p. 472.
3. Bruhat and Maréchal, *op cit.*, p. 264.
4. J. Dyson, *Proceedings of the Physical Society*, **B 62,** 565 (1949).
5. M. Françon, *Revue d'Optique* 3, 3 (1950).

Received April 24, 1973

The author is located at the IBM Thomas J. Watson Research Center, Yorktown Heights, New York 10598.